

Flight Calibration of Flow Angularity Sensors on Tejas Using Advanced Parameter Estimation Techniques

Amitabh Saraf^{*1}, G. Kumaresan[#]

^{*}Sc/Engr 'F', IFCS, Aeronautical Development Agency, Bangalore

[#]Scientist 'C', National Aerospace Laboratories, Kodihalli, Bangalore

Abstract

Calibration of flow angularity sensors forms a very significant part of the flight tests carried out on a new aircraft. This paper describes the advanced parameter estimation techniques adopted for calibrating these sensors on Tejas. Flight path reconstruction procedures have been used to reconstruct the flight trajectories and compute the free stream Angle of Attack and Angle of Sideslip. The errors between measurements and the free stream values are then modeled. Optimization techniques are used to estimate the free parameters of the models to minimize the error. Flight data collated over a large number of maneuvers on seven different aircraft configurations have been used simultaneously. The results of the calibrations have been very consistent and typical results are presented in this paper.

Keywords: airdata calibration, flight test, Tejas

1. INTRODUCTION

Tejas (LCA) is India's first indigenous combat aircraft with a full authority, quad-redundant, digital fly-by-wire flight control system. The aircraft is aerodynamically unstable in the longitudinal axis and is artificially stabilized using flight control laws. These control laws are implemented in the on-board quad-redundant digital flight control computers. Airdata system onboard the aircraft provides vital information on various flight parameters like airspeed, altitude, Angle of Attack (AOA), Angle of Side Slip (AOSS) etc. to the control laws and to the pilot through cockpit displays. AOA and AOSS are used as primary feedback signals, and airspeed and altitude are used as important gain-scheduling parameters within the control laws. So, reliable and accurate air data measurements are very important for the control laws to guarantee stability and performance of the aircraft over the complete flight envelope. Airdata parameters are also extensively used by various aircraft subsystems including the mission management and engine control systems.

Flow angularity sensors on Tejas are used to measure AOA and AOSS of the aircraft in flight. There are five primary flow angularity sensors on Tejas. There are two AOA Vanes mounted on either side of the front fuselage as the main sources for AOA measurement. Two side airdata probes also mounted on either side of the fuselage, measure local flow angles through differential pressure measurements (called ' $P\alpha_1$ - $P\alpha_2$ '). Figure 1 is a schematic diagram showing the various pressure ports on an airdata probe and gives the relationship between the differential pressures and the local flow angle. Combined together these local flow angles from the two probes can be used to compute both AOA and AOSS. Nose probe provides another source for AOSS through differential pressure measurement (called ' $P\beta_1$ - $P\beta_2$ '). In addition to these primary sensors, on two of the test aircraft a flight test boom was also mounted which provided two additional sources for AOSS and one additional source for AOA measurement. (The boom replaced the existing nose probe and hence $P\beta_1$ - $P\beta_2$ measurements were not available when the boom was installed.) A large variety of sensors have been used for the measurement of local flow angularity on different aircraft. Ref. [1] gives a good description of typical airdata sensors.

^{*}am.saraf@gmail.com (First author)

[#]gkumar@css.nal.res.in (Second Author)

¹Corresponding Author

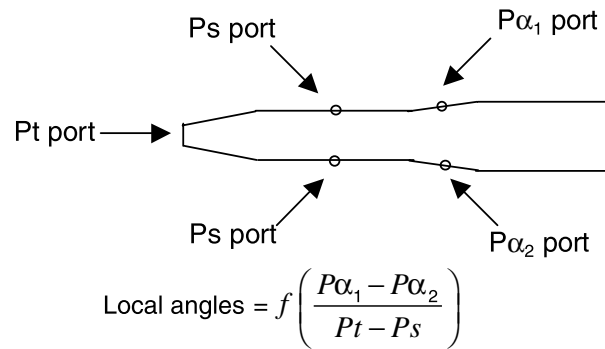


Figure 1. Schematic of port locations on the airdata probe

Most of the airdata sensors are mounted outside the aircraft and very close to the body. As a result, they measure pressures and flow angles in local flow fields near the aircraft body and are significantly different from the free stream values. All the measured quantities from airdata sensors need to be corrected by the airdata computers to obtain the free stream information. For the first few flights of Tejas, these corrections were implemented based on models developed using Computation Fluid Dynamics (CFD) methods or using wind tunnel data. With the progression of flight tests the correction models were updated using flight test data. This process of updating the airdata correction models is termed as airdata calibration and has been well studied in the literature. References [1,2,3] discuss some of the well-known methods for airdata calibration.

For Tejas, flow angle corrections are nonlinear functions of free stream AOA, AOSS and Mach numbers, and are represented using three dimensional correction tables. Airdata calibration process results in updating of these tables. Ref. [4] gives an overview of the earlier efforts for airdata calibration of Tejas using conventional methods. There were several issues with conventional techniques, most notably, true AOA computation was not possible for coupled maneuvers like wind-up-turns, and true AOSS showed a significant drift for long duration maneuvers like Steady Heading Side-Slip (SHSS) resulting in poor calibration of AOSS. The conventional techniques are also inadequate when the aircraft flies at higher AOA, where airdata corrections as well as aircraft aerodynamic characteristics become highly nonlinear. So in place of conventional techniques, advanced techniques like Flight Path Reconstruction (FPR) and parameter estimation have been adopted for calibration.

FPR technique (or often called kinematic consistency technique) has been described in detail in Ref. [5]. It is a prerequisite for estimating aero-data coefficients from flight data. Ref [6-7] describes the application of FPR technique for airdata calibration.

The present paper describes FPR and parameter estimation methods and presents several calibration results for both AOA and AOSS sensors. We also discuss issues related to estimation of bias in vane measurements to the actual installation errors of the vane. Using the results generated over a large number of maneuvers on seven different aircraft /configurations, it has been confirmed that airdata system of Tejas is capable of measuring the flow angles to the desired accuracy.

2. FLIGHT PATH RECONSTRUCTION

The basic aim of FPR is to analytically reconstruct the aircraft trajectory using reliable and accurate linear acceleration and angular rate measurements by the inertial sensors mounted on the aircraft. As the trajectory is reconstructed offline on the computer, AOA and AOSS computed from this trajectory are used as the true AOA and AOSS for the calibration of airdata sensors. Fig. 2 shows a block schematic of the process of FPR.

2.1. State Equations

In the FPR procedure adopted here, three linear accelerations along the body axes A_x , A_y , A_z and three angular rate measurements along the body axes p , q , r from the aircraft are used to compute the trajectory. The kinematic equations in Eq. (1) are used (see Ref. [5]).

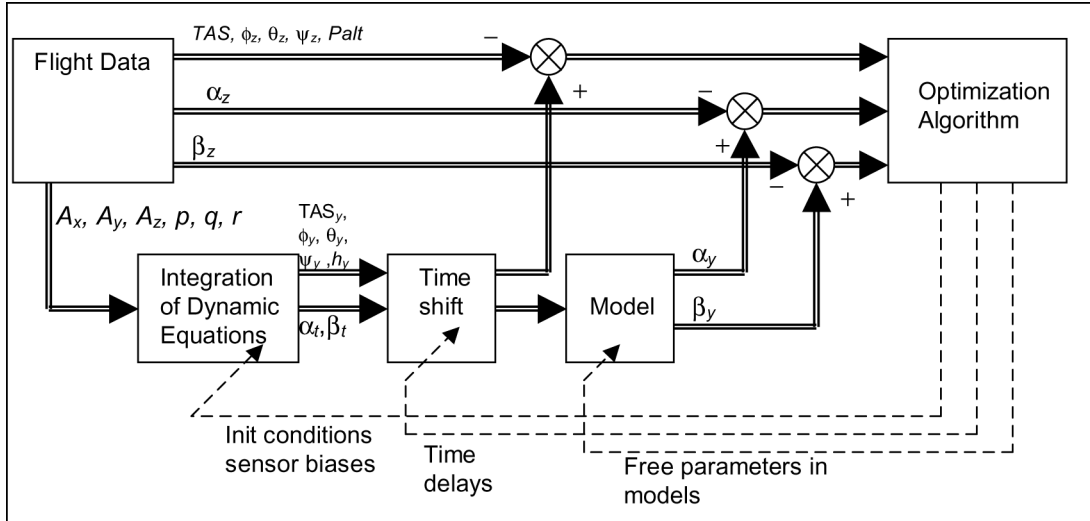


Figure 2. Block schematic of the FPR process

$$\begin{aligned}
 \dot{u} &= -(q - \Delta q)w + (r - \Delta r)v - g \sin \theta + (A_x - \Delta A_x) \\
 \dot{v} &= -(r - \Delta r)u + (p - \Delta p)w + g \cos \theta \sin \phi + (A_y - \Delta A_y) \\
 \dot{w} &= -(p - \Delta p)v + (q - \Delta q)u + g \cos \theta \cos \phi + (A_z - \Delta A_z) \\
 \dot{\phi} &= (p - \Delta p) + (q - \Delta q) \sin \phi \tan \theta + (r - \Delta r) \cos \phi \tan \theta \\
 \dot{\theta} &= (q - \Delta q) \cos \phi - (r - \Delta r) \sin \phi \\
 \dot{\psi} &= (q - \Delta q) \sin \phi \sec \theta + (r - \Delta r) \cos \phi \sec \theta \\
 \dot{h} &= u \sin \theta - v \cos \theta \sin \phi - w \cos \theta \sin \phi
 \end{aligned} \tag{1}$$

These equations are integrated and a trajectory is obtained in terms of the states u, v, w (linear velocities), ϕ, θ, ψ (Euler Angles) and h (altitude) starting from the corresponding free initial states. The following are taken as the free variables for optimization in Eq. (1): $\Delta A_x, \Delta A_y, \Delta A_z, \Delta p, \Delta q, \Delta r$ (small biases in the sensor measurements) and $u_0, v_0, w_0, \phi_0, \theta_0, \psi_0$ (the initial condition of the trajectory). h_0 is normally kept the same as measured h at the beginning of the trajectory.

To ensure that this trajectory correctly matches the measured aircraft trajectory an optimization problem is formulated. The cost function for the optimization is the least square error between the measurements and the outputs of the state equations as described below.

2.2. Measurement Equations

The measurement parameters chosen for FPR are

$$Z = [\phi_z, \theta_z, \psi_z, TAS, Palt, \alpha_{zl}, \alpha_{zr}, \alpha_{xp}, \alpha_{xb}, \beta_{xp}, \beta_{xb}, \beta_{bu}, \beta_{bl}]$$

Here ϕ_z, θ_z, ψ_z are the measured Euler angles from Inertial Navigation System, TAS is the true air speed obtained from calibrated pressures and static temperature measurements and $Palt$ is the pressure altitude obtained from the calibrated static pressure measurements.

There are seven different sources of AOA/AOSS measurements that have been flown on Tejas and that need to be calibrated. The following list describes these measurements

α_{zl}, α_{zr} : While the left and right AOA vane sensors actually measure the local flow angles (called α_{lm}, α_{rm} respectively), these are not directly used as measurements. The local angles are first corrected to obtain the left and right free stream vane angles using the baseline correction table f_v generated by the CFD/Wind tunnel methods. These baseline corrected angles are called α_{zl} and α_{zr} respectively.

α_{zsp} : As above, we call α_{lsp} , α_{rsp} as the measured left and right probe local flow angles (obtained from the $P\alpha_1$ - $P\alpha_2$ measurements as given by the equation in Fig 1). The combination of these left and the right probe local angles are corrected to obtain the free stream angle α_{zsp} . The conversion from measured to free stream value has been done using baseline correction tables f_{sp} generated by the CFD/Wind tunnel methods.

α_{zb} : AOA measured by the vane sensor mounted on the flight test boom.

β_{zsp} : This is the AOSS estimate provided by the combination of α_{lsp} and α_{rsp} , using baseline correction tables f_{sp} similar to α_{sp} .

β_{znp} : This is the estimate of AOSS obtained from ' $P\beta_1$ - $P\beta_2$ ' measurements from the nose probe using correction tables f_{np} provided by the manufacturer of the short nose probe.

β_{zbl} , β_{zbu} : These are the AOSS measured by the lower and the upper vane mounted on the flight test boom.

The equations for computation of the above variables are given below.

$$\begin{aligned}\alpha_d &= f_v(\alpha_m, M) \\ \alpha_x &= f_v(\alpha_m, M) \\ \alpha_{zsp} &= f_{sp}(\alpha_{lsp}, \alpha_{rsp}, M) \\ \beta_{zsp} &= f_{sp}(\alpha_{lsp}, \alpha_{rsp}, M) \\ \beta_{znp} &= f_{np}(p\beta_1 - p\beta_2, \alpha_d, \alpha_x, M_m)\end{aligned}\quad (2)$$

where M and M_m are the free stream mach number and mach measured obtained using Pt and Ps measured by the nose probe respectively.

2.3. Observation Equations

The observation variables are

$$Y = [\phi_y, \theta_y, \psi_y, TAS_y, h_y, \alpha_{yl}, \alpha_{yr}, \alpha_{ysp}, \alpha_{yb}, \beta_{ysp}, \beta_{ynp}, \beta_{ybu}, \beta_{ybl}]$$

ϕ_y , θ_y , ψ_y are obtained from the states ϕ , θ , ψ . In reality, measurements from INS (ϕ , θ , ψ) are quite accurate. However, there could be time shifts in recording these variables in various Data Recording Units installed on the aircraft. For accurate matching of the trajectories these time shifts also need to be estimated. The amount of time shift necessary for each variable is taken as a free parameter in the optimization and included in the reconstructed trajectory accordingly. Time shifts are implemented in the following manner

$$y(t, \tau) = y(t - \tau_y) \quad (3)$$

where τ corresponds to the time shift to be estimated and y is an observation variable from Y .

For the other parameters, using u , v , w (which are the states of the computed trajectory), we define

$$\begin{aligned}TAS_t &= \sqrt{u^2 + v^2 + w^2} \\ \alpha_t &= \tan^{-1}\left(\frac{w}{u}\right) \\ \beta_t &= \sin^{-1}\left(\frac{v}{TAS}\right)\end{aligned}\quad (4)$$

where the subscript t refers to the true values. The parameters α_t , β_t calculated above are at the C.G of the aircraft, which are converted to various sensor locations using a kinematic correction (kc) term.

$$\begin{aligned}\alpha_{si} &= \alpha_t + kc\alpha_i \\ \beta_{sj} &= \beta_t + kc\beta_j\end{aligned}\quad (5)$$

Here $i \in \{lv, rv, sp, ba\}$, $j \in \{sp, np, bu, bl\}$. Subscript lv denotes the left AOA vane, rv the right AOA vane, sp the side probe, ba the boom alpha vane, np the nose probe, bu the boom beta upper vane and bl the boom beta lower vane.

Kinematic correction is based on the sensor position location and the angular body rates. For example the kc corrections for the side probe is as the following.

$$\begin{aligned}kc\alpha_{sp} &= \frac{(X_s - X_{cg})q}{TAS_t} + \frac{(Y_s - Y_{cg})p}{TAS_t} \\ kc\beta_{sp} &= \frac{(Z_s - Z_{cg})p}{TAS_t} + \frac{(X_s - X_{cg})r}{TAS_t}\end{aligned}\quad (6)$$

where X_s, Y_s, Z_s are the x, y and z distances of the side probe sensor location from a reference point. Similarly X_{cg}, Y_{cg}, Z_{cg} are the x, y and z distances of the current aircraft C.G from the same reference point.

α_{si} and β_{si} obtained using Eq. (5) provide a very accurate estimate of true AOA and AOSS even in the presence of steady winds. This is because by allowing the initial conditions u_0, v_0, w_0 to be free, FPR method is able to estimate and include average winds during the maneuver into the reconstructed trajectory. Now AOA, AOSS measurements listed in Z would not match α_{si} and β_{si} exactly. The basic purpose of calibration using flight path reconstruction is to model the differences between the corresponding measured and observed quantities. For this we define ‘models’ that serve dual purposes: (i) matching the trajectory with flight measurements and (ii) providing a procedure to model the differences. Table 1 lists the various models used for calibration of estimates.

Table 1. Models for AOA measurements

Observation variable	Model	Free parameters for optimization
α_{yl}	$f_1(\alpha_{slv}) + f_2(\alpha_t) * \beta_{slv} + b_l$	f_1, f_2 are table look up functions with values at fixed break points as free variables, b_l is the left vane bias
α_{yr}	$f_1(\alpha_{srv}) + f_2(\alpha_t) * \beta_{srv} + b_r$	f_1, f_2 same as above, b_r is the right vane bias
α_{ysp}	$f_3(\alpha_{zsp}) + b_{sa}$	f_3 is a similar table as above, b_{sa} is side probe AOA bias
α_{yba}	$k_{ba} \alpha_{sba} + b_{ba}$	k_{ba} is the scale factor and b_{ba} is the nose boom AOA bias
β_{ysp}	$f_4(\alpha_{zsp}) \beta_{zsp} + b_{sb}$	f_4 is a similar table as above, b_{sb} is side probe AOSS bias
β_{ynp}	$f_5(\alpha_t) \beta_{snp} + b_n$	f_5 is a table look up as above, b_n is nose probe AOSS bias
β_{ybu}	$k_{bu} \beta_{sbu} + b_{bu}$	k_{bu} is the scale factor and b_{bu} is upper vane boom AOSS bias
β_{ybl}	$k_{bl} \beta_{sbl} + b_{bl}$	k_{bl} is the scale factor and b_{bl} is lower vane boom AOSS bias

The complete observation equations, which are matched with the measurement equations, are given below.

$$\begin{aligned}
\phi_y &= \phi(t, \tau_\phi) \\
\theta_y &= \theta(t, \tau_\theta) \\
\psi_y &= \psi(t, \tau_\psi) \\
TAS_y &= TAS_t(t, \tau_{TAS}) \\
h_y &= h(t, \tau_h) \\
\alpha_{yl} &= f_1(\alpha_{sl}(t, \tau_l)) + f_2(\alpha_t) * \beta_{sl}(t, \tau_l) + b_l \\
\alpha_{yr} &= f_1(\alpha_{sv}(t, \tau_r)) + f_2(\alpha_t) * \beta_{sv}(t, \tau_r) + b_r \\
\alpha_{ysp} &= \alpha_{sp}(t, \tau_{sp}) + f_3(\alpha_{zsp}(t, \tau_{sp})) + b_{sa} \\
\alpha_{yb} &= \alpha_{sba}(t, \tau_b) + k_{ba} * \alpha_{sba}(t, \tau_b) + b_{ba} \\
\beta_{ysp} &= \beta_{sp}(t, \tau_{sp}) + f_4(\alpha_{zsp}) * \beta_{zsp} + b_{sb} \\
\beta_{ynp} &= f_5(\alpha_t) * (\beta_{snp}(t, \tau_{np}) + b_n) \\
\beta_{ybu} &= \beta_{sbu}(t, \tau_{bu}) + k_{bu} * \beta_{sbu}(t, \tau_{bu}) + b_{bu} \\
\beta_{ybl} &= \beta_{sbl}(t, \tau_{bl}) + k_{bl} * \beta_{sbl}(t, \tau_{bl}) + b_{bl}
\end{aligned} \tag{7}$$

The total number of free parameters used for optimization for a single maneuver are: 6 sensor biases, 6 initial conditions, about 12 time delays and about 70 model parameters as given in Table 1.

2.4. Integrated Environment for FPR

Airdata calibration for Tejas using FPR techniques has been carried out using Estima software package [8]. Estima has been developed at the Institute of Flight Systems, Braunschweig, Germany and is a dedicated software tool for system identification studies. The software incorporates various advanced parameter estimation techniques like filter error method and extended Kalman filter besides the classical output error and least square methods. It can handle large amount of data (up to 80000 points from 70 flight maneuvers). Estima is installed under LINUX operating system in a user friendly environment created with the X-windows organizer.

The trajectory matching has been done using the Output Error Method [5]. The cost function was derived using Maximum Likelihood Principle and optimization has been carried out using Gauss Newton method. Fourth order Runge Kutta method was used for the integration of the dynamic equations Eq. (1) to compute the trajectory.

3. FLIGHT TEST DATA

Tejas has completed over one thousand flights on seven different prototypes. Several of these flights have been used for generation of data for airdata calibration. Since airdata corrections have been found to vary with Mach number, AOA and AOSS, care has been taken during the planning of flight tests to obtain a good coverage these parameters. A large number of dedicated maneuvers were planned and flown which include maneuvers like pull ups and push downs, roller coasters, pitch doublets and 3211 maneuvers, steady heading sideslips, pull-up with rudder doublets, level accelerations and decelerations, and wind-up turns etc.

Flight data for calibration is acquired from several sources like, (i) digital flight control computer data from Data Recording Unit (DRU), (ii) inertial velocities data from INS, and (iii) height information data from post-processed DGPS. As a first step, data segments for relevant maneuvers are extracted from the entire sortie data. Since data is obtained from disparate sources, the recorded parameters are pre-processed to a common time base. A special software tool has been created that extracts maneuver data from relevant streams of data sources and stores the data in ASCII format for

use within Estima. For ease of estimation, the maneuvers are sorted out according to the average Mach number value during the maneuver. So in the beginning those maneuvers which show large Mach number variations are not considered. For each Mach number 60-70 maneuvers have been selected which were flown on three different prototype aircraft with nose probes and two aircraft with nose probe and nose boom each flown at different points of time. Calibration of airdata sensors has been carried out taking into account data from all five aircraft. From preliminary studies it has been established that other than undercarriage position, any other change in aircraft configuration like extension of slats, airbrakes etc does not influence the flow near the AOA, AOSS sensors. As a result, most of the calibration has been carried out in up and away conditions with undercarriage retracted. To study the influence of undercarriage extension on flow angularity, several maneuvers in approach, take off and up-and-away flight phases with undercarriage down have also been separately used for calibration.

4. CALIBRATION RESULTS

Among all the airdata signals that are used by the control laws for feedback, AOA is the most important. Airdata algorithms compute AOA signal for feedback from the two AOA vanes (α_{zl} , α_{zr}) only. AOA from side probes is used only as a monitoring signal to detect a mechanically failed vane. AOA from nose boom is currently only used for calibration and is not being used for feedback. As a result the most stringent requirement for calibration is for the vane AOAs (α_{zl} , α_{zr}). The desired 3-sigma accuracy for these signals is ± 0.5 deg. For the side probe AOA (α_{zsp}) desired 3-sigma accuracy for these signals is ± 1 deg as that would help in fixing the threshold for failure detection.

Among the AOSS signals, β_{zsp} is used as a monitoring signal, while β_{znp} is planned to be used as a feedback signal at lower AOA. (This is because β_{znp} nose probe is known to have certain indeterminacy problems at higher AOA). AOSS signals from the nose boom are currently planned for calibration only. The desired 3-sigma accuracies for β_{zsp} , β_{znp} are ± 1 deg, and ± 0.5 deg at lower AOA, respectively.

Fig. 3 shows the time history match for several maneuvers at Mach number 0.6. It can be seen that the outputs of AOA, AOSS models for all the sensors have matched the measured quantities very well. For a consistent calibration it is important to have a set of maneuvers that show a good coverage of AOA, AOSS. Since integration of dynamic equations is required in FPR, it is good to choose

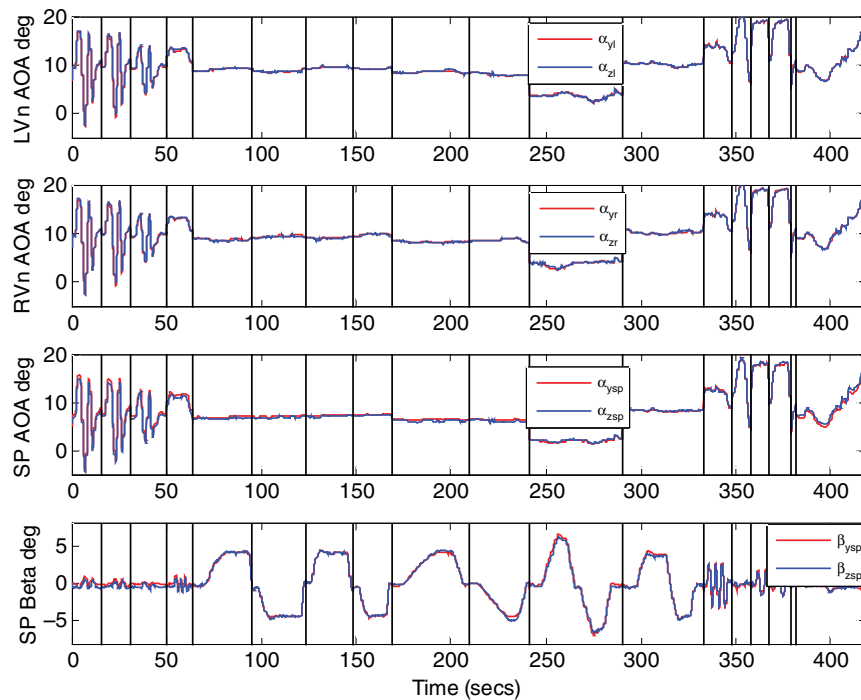


Figure 3. Time response match for some parameters for about 18 maneuvers at Mach number 0.6

maneuvers that are not longer than 30-40 seconds duration. In case of steady heading sideslips, the maneuvers have been split into multiple maneuvers of 30-40 seconds each. This enables a good match and consistent calibration. The errors of calibration are obtained by cross-plotting difference of measured and model quantities with respect to the measured quantity.

4.1. Vane AOA Calibration

For vane AOA correction model, two table look up corrections f_1 and f_2 and one bias correction b_l/b_r are used (see Eq. (7)). It has been found that three sources of error contribute to the bias corrections on vanes: (i) installation error (which we shall call as the 'installation bias'), (ii) local-to-free-stream correction model bias error (which means that zero local angle does not give zero free stream AOA), and (iii) the extra bias that is noticeable when undercarriage is extended. While it is possible to isolate the undercarriage effects by choosing maneuvers properly, the other two errors are difficult to isolate. As can be seen in Table 1, FPR process does help in obtaining b_l and b_r as biases for the vanes but we still need to apportion these bias values between installation bias for each aircraft and the consistent error attributable to the correction model. The individual installation bias errors for each aircraft are presently planned to be corrected within the flight control computer independently for each aircraft.

Fig. 4 shows a plot of average of b_l and b_r (which are obtained by carrying out FPR process) against Mach numbers for the five aircraft used for study. The mean value for the five aircraft at each Mach number is also plotted. This mean value is regarded as the update required to the correction model and difference of $(b_l + b_r)/2$ and the mean for each aircraft is taken as the mean installation bias. Individual left and right installation biases are calculated from the mean installation bias. For ease of calculation of installation biases for future Tejas aircraft, the mean installation bias is calculated only at Mach number 0.5 and assumed constant for other Mach numbers. The future Tejas aircraft can now be maneuvered at Mach no. 0.5 in the first few flights and an accurate value of installation biases can be found.

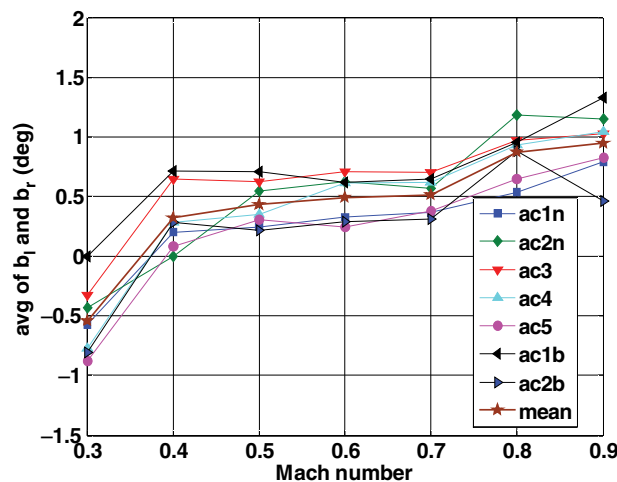


Figure 4. Average of biases b_l and b_r estimated for the five aircraft

After calculating installation biases, FPR process is run again with b_l and b_r values fixed for each aircraft and the free parameters in f_1 and f_2 functions are again estimated. These parameters now help model the updates required to the local-to-free-stream correction model, which would be valid for all the aircraft. The same process (with b_l and b_r values fixed for each aircraft) is carried out for all undercarriage down maneuvers. This helps in estimating the undercarriage down corrections also. Fig. 5 shows a cross-plot of $(\alpha_{zl} - \alpha_{yl})$ v/s α_{yl} and $(\alpha_{zr} - \alpha_{yr})$ v/s α_{yr} at a typical Mach number for about 70 maneuvers taken from the different aircraft. It can be seen that the difference between the model outputs and measurements are very small, and the 3-sigma errors (as given in Table 2) are well within the desired accuracy requirements. Fig. 6 shows the plots of final updates that have to be made to the local-to-free-stream correction model at different Mach numbers. The figure also shows the update to the model required when undercarriage is extended. With the correct installation bias and the updated correction model, the vanes provide a very accurate estimate of AOA.

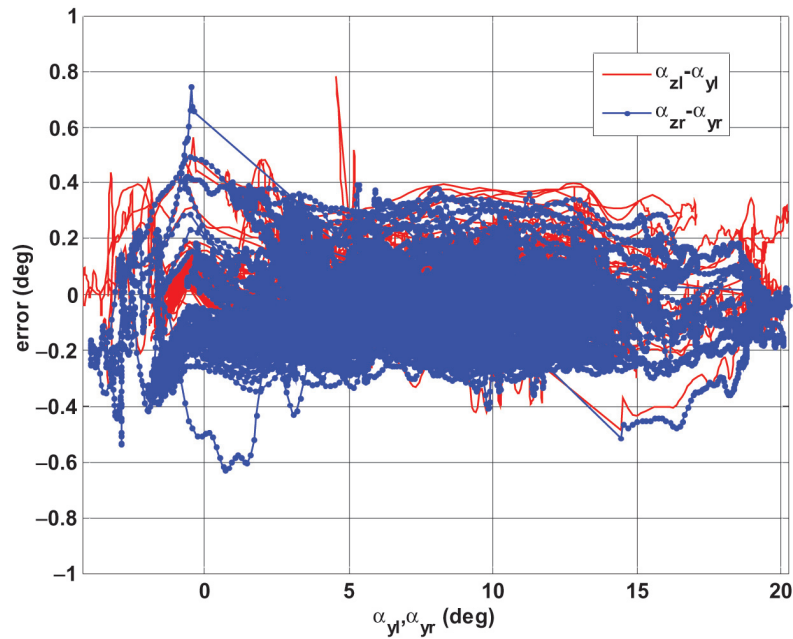


Figure 5. Cross plot of error between model and measurement for left and right vane AOA at $M = 0.6$

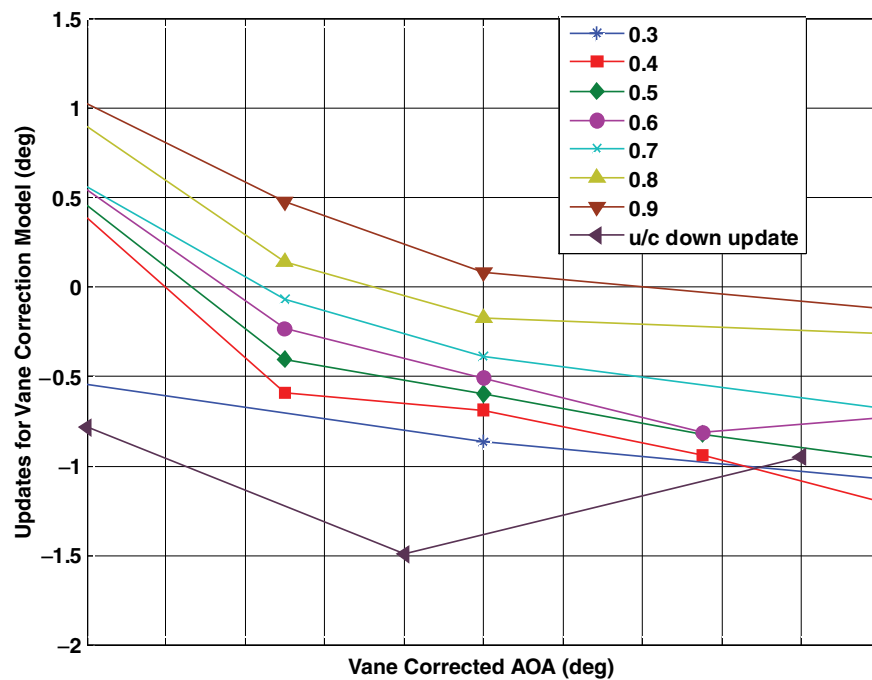


Figure 6. Updates required for the vane correction tables for different Mach numbers

4.2. Calibration of Other Sensors

The side probes and the nose probe also have correction models as well as installation errors but since these are not primary feedback signals, separate installation biases would not be implemented for each aircraft in the flight control computer.

Figs. 7 shows the cross plots for difference of model output and measurement for nose probe AOA. The figure shows the increase in modeling errors at higher AOAs at Mach number 0.3. The errors do

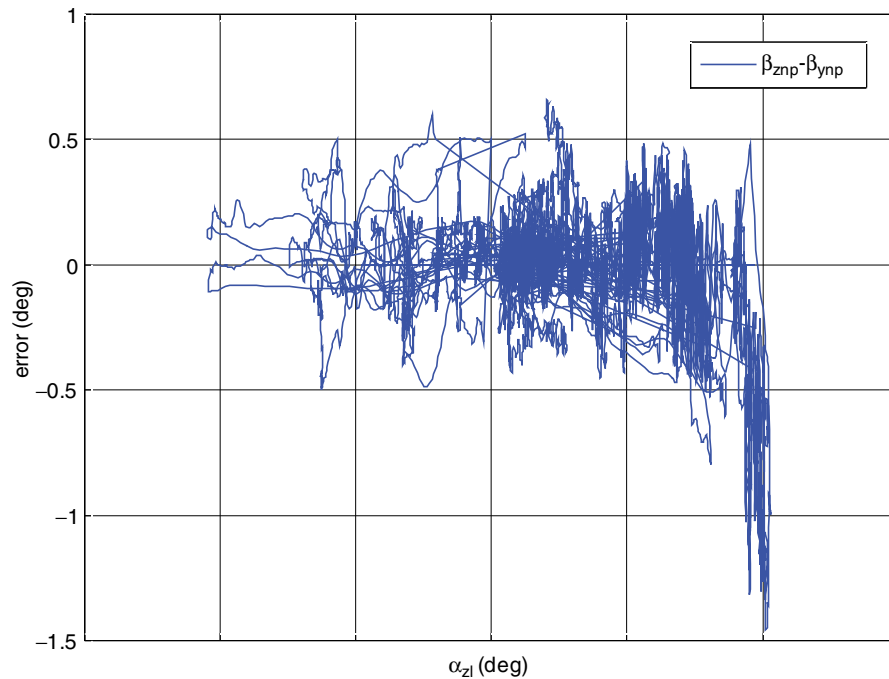


Figure 7. Increase of Nose Probe AOSS error with increase in AOA at $M = 0.3$

not have any specific trends with any parameter and appear as large noise, making it impossible to model. Based upon such plots it is possible to define ranges of AOA upto which nose probe AOSS can be used for feedback. These plots also indicate that there is a need for another source for AOSS for feedback at higher AOA.

Fig. 8 shows the updates that should be made to the side probe AOA correction table to improve the accuracy of measurement. Though the estimation of model parameters have been carried out for

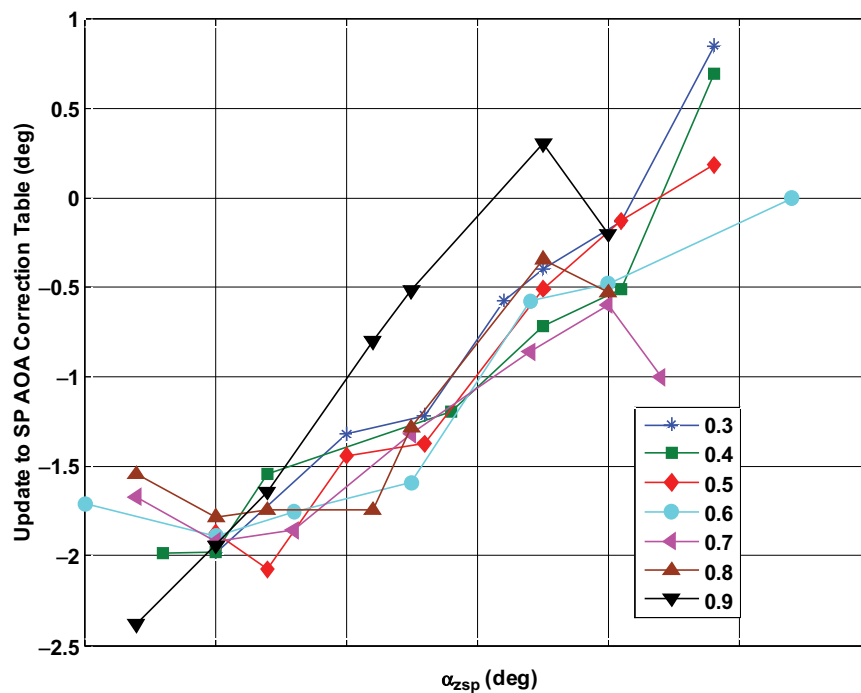


Figure 8. Updated required for Side probe AOA tables for different Mach numbers

different Mach numbers one at a time, the updates required for the correction tables are quite consistent over the entire range of Mach numbers.

Table 2 lists the 3-sigma accuracy numbers for all the modeling errors for all the sensors at various subsonic Mach numbers. It can be clearly seen that all the sensors meet the desired accuracy requirements. The best sensors of course turn out to be the nose boom AOA and AOSS vanes. This confirms that with some limited calibration, nose boom sensors can be used to obtain true AOA, AOSS and hence used as the reference for calibrating the other sensors.

Table 2. 3-sigma values for calibration errors of various AOA/AOSS sensors (in deg.)

	Left Vane	Right Vane	Side Probe	Nose Boom	Nose Probe	Side Probe	Nose Boom
Mach	AOA	AOA	AOA	AOA	AOSS	AOSS	AOSS
0.3	0.38	0.37	0.78	0.16	0.68	0.89	0.18
0.4	0.26	0.27	0.69	0.11	0.48	0.77	0.17
0.5	0.35	0.35	0.69	0.17	0.35	0.63	0.33
0.6	0.28	0.34	0.81	0.25	0.26	0.79	0.18
0.7	0.39	0.42	0.96	0.18	0.44	0.68	0.22
0.8	0.38	0.35	0.77	0.11	0.27	0.74	0.20
0.9	0.41	0.44	0.77	0.15	0.37	0.67	0.29

5. CONCLUSIONS

Calibration of flow angle sensors forms a very important part of flight testing of a new aircraft and is a prerequisite for flight envelope expansion. This paper outlines the techniques adopted for calibrating these sensors on Tejas. Flight path reconstruction using a dedicated parameter estimation package like Estima yields very consistent calibration results as shown in the paper. Post calibration the flow angle sensors on Tejas are able to provide the desired accuracy of measurements over the design envelope.

6. ACKNOWLEDGEMENTS

The authors are grateful to Mr Shyam Chetty, Project Director (CLAW), National Aerospace Laboratories and Dr. Girish S. Deodhare, Associate Project Director (CLAW), Aeronautical Development Agency for their support and encouragement to carry out this work. Authors would also like to thank Dr R.V. Jategaonkar, Senior Scientist, DLR, Germany for his guidance for this work.

7. REFERENCES

- [1] Gracey, W., "Summary of Methods of Measuring Angle of Attack on Aircraft", *NACA Technical Note 4351*, Aug. 1958.
- [2] Huston, W. B., "Accuracy of Airspeed Measurements and Flight Calibration Procedures", *NACA Report 919*, May 1946.
- [3] Haering Jr., E. A., "Air Data Calibration of a High-Performance Aircraft for Measuring Atmospheric Wind Profiles", *NASA Technical Memorandum 101714*, Jan 1990.
- [4] Saraf, A., Viswanathan, S., "Flight Testing and Calibration of Tejas Airdata System", *IFTS2008-P-28*, International Flight Test Seminar, ASTE, Bangalore, Feb 14-15, 2008.
- [5] Jategaonkar, R.V., *Flight Vehicle System Identification: A Time Domain Methodology*, Vol. 16, AIAA Progress in Astronautics and Aeronautics, AIAA Reston, VA, Aug 2006.
- [6] Keskar, D. A. and Klein, V., "Determination of Instrumentation Errors from Measured Data Using Maximum Likelihood Method", *AIAA 80-1602*, 1980.
- [7] Parameswaran, V., Jategaonkar, R. V. and Press, M., "Calibration of Five-Hole Probe from Dynamic and Tower Fly-By Maneuvers", *Journal of Aircraft*, Vol. 42, No. 1, 2005, pp. 80-86.
- [8] Jategaonkar, R.V., Thielecke, F., "ESTIMA—An Integrated Software Tool for Nonlinear Parameter estimation", *Journal of Aerospace Science and Technology*, Vol. 6, No. 8, 2002, pp. 565-578

